UNCERTAINTY ANALYSIS OF FAILURE PROBABILITY PREDICTIONS FOR BRITTLE FRACTURE

H. RIESCH-OPPERMANN[1] & S. ROUDI[1] & T. ERBACHER[2]
[1]Forschungszentrum Karlsruhe, IMF II, P.O.Box 3640, D-76021 Karlsruhe, Germany
[2]Karlsruhe University, IWK I, Kaiserstr. 12, D-76131 Karlsruhe, Germany

ABSTRACT

Reliability analysis of ceramic components under stationary or transient loading is generally performed on the basis of a Finite Element stress analysis from which the failure probability according to the multi-axial Weakest Link theory is calculated with the help of a suitable post-processing routine. We use the STAU post-processing routine and the general purpose Finite Element code ABAQUS. Due to scatter in the material parameters, the resulting failure probability is also prone to statistical uncertainties. We present a method of assessing this scatter using so-called resampling simulation methods. We obtain confidence intervals for the failure probability. In a toy example using a four-point bend specimen, the effect of pooling (i.e. grouping of results from different experiments by suitable scaling procedures) on numerical result and scatter of failure probability is demonstrated. Here, pooling is done using results of inert strength measurements at various temperatures and scaling to room temperature values. While the confidence interval of the failure probability for the pooled data set gets smaller as expected from the increased sample size, its upper bound remains stable which is a surprising result. A more realistic example deals with a ceramic component in a model clutch under thermo-mechanical frictional loading. It is investigated, if the results of the toy example can be reproduced in this more complicated case. As a first step, the local risk of rupture is calculated which leads to the identification of the most critical regions of the component. As a second step, resampling confidence intervals for the failure probability are determined. As resampling data base, we use inert strength values at different temperatures as well as material data for sub-critical crack propagation.

1 INTRODUCTION

It is common practice to use the multi-axial Weibull theory [1]-[4] and its extensions [5] to calculate the failure probabilities of ceramic components. Codes are currently available which allow a probabilistic design under constant [6] or general time-dependent loading [7]. Temperature-dependent material properties can also be taken into account [7]. Due to the scatter in fracture behaviour and sub-critical crack propagation of ceramic materials, calculated failure probabilities are also prone to statistical uncertainties. Because of the complex and nonlinear relation between material parameters and failure probability that is usually obtained using numerical integration of a Finite Element stress field, standard methods of establishing confidence intervals are not available because no sampling distribution for the failure probability P_f is available. Also material data are sometimes difficult and expensive to obtain, especially if temperature-dependent data are required or in the case of time-consuming lifetime measurements [8]. It is then desirable to have ways of using data from different experiments for a common purpose. This so-called pooling procedure is a way of reducing statistical scatter because of an increase in the sample size. However, care has to be take that pooling does not lead to inhomogeneous samples. As an example, we will show how inert strength data obtained at various temperatures can be used to reduce scatter in the failure probability estimation at a selected temperature level. In the following section two, a short review of the relations used for failure probability calculation based on the multiaxial Weakest Link approach will be given. Section three contains the basic framework for uncertainty assessment of material parameters and failure probability, namely confidence intervals based on bootstrap re-

sampling. In section four, a toy example will first be given which demonstrates the basic approach of pooling and uncertainty assessment. A second example which is based on numerical analysis of the stress and temperature distribution of a ceramic plate in a clutch test rig shows the range of scatter in a more realistic case and provides a validation of the approach. Validation is obtained both with respect to failure probability levels and with respect to local risk of rupture calculations which are both obtained by the STAU post-processing routine [7] for the general purpose Finite Element code ABAQUS.

2. FAILURE PROBABILITY

The time-dependent failure probability $P_f(t)$ for a ceramic component under transient loading that fails due to the presence of volume flaws is given by the following equation [5]:

$$P_f(t) = 1 - \exp\left[-\frac{1}{V_0} \int_V \frac{1}{4\pi} \int_\Omega \left(\max_{\tau \in [0,t]} \left\{ \left[\left(\frac{\sigma_{eq}(\tau)}{\sigma_0} \right)^{n-2} + \Psi \right]^{\frac{1}{n-2}} \right\} \right)^m d\Omega \, dV \right] \quad (1)$$

with

$$\Psi = \frac{\sigma_0}{B} \int_0^\tau \left(\frac{\sigma_{eq}(t')}{\sigma_0} \right)^n dt' \quad (2)$$

describing the contribution from sub-critical crack growth with crack growth parameters n and B to P_f. The parameters σ_0 and m denote the Weibull parameters for the inert strength distribution, σ_{eq} is the equivalent stress for the fracture mechanics description of natural cracks, usually the normal stress on the crack faces, and V_0 is a unit volume. The quantity Ψ defined in Eqn. (2) describes the contribution of sub-critical crack propagation on P_f. For $\Psi=0$, the probability for spontaneous fracture is obtained. Under transient loading, the maximum of the load is relevant for fracture according to the braces in eqn (1). Integration has to be performed over the component volume V and over all possible orientations of cracks Ω. Generalisation of Eqn. (1) for surface flaws is obvious.

The material parameters m, σ_0, n, and B are prone to statistical scatter. Therefore, the numerical value of P_f has only limited evidence because scatter in material parameters transfers to scatter in the failure probability P_f so that an interval estimate of P_f is required.

3. CONFIDENCE INTERVALS

Interval estimates of P_f are difficult to obtain by analytical methods because of the complex relation to material parameters given in Eqns. (1), (2), where the respective contributions from sub-critical crack propagation (parameters n and B) and spontaneous fracture (parameters m and σ_0) are not independent, as can be seen from the fact that the respective terms in Eqns. (1), (2) cannot be separated. Dependence of the various parameters makes it impossible to combine confidence intervals for the material parameters and to obtain a resulting confidence interval for P_f. Moreover, while appropriate confidence intervals exist for parameters m and σ_0 [9], they are not available for parameters n and B. Fortunately alternative approaches exist and we have chosen the bootstrap resampling approach [10] which allows to obtain the empirical cumulative distribution function for P_f from random sampling results generated from the available inert strength and crack propagation data base from which material data estimates were obtained [11]. A sketch of the bootstrap resam-

pling procedure is shown in Fig. 1. In our case, we use the original data points, obtain one set of material parameters (m, σ_0, n, and B) and one estimate of the failure probability, P_f. Then, using a large number of copies of the original data set, the so-called bootstrap population, we draw a number of bootstrap samples by random sampling from the bootstrap population and obtain a bootstrap replication of the parameter set (m, σ_0, n, and B) for each bootstrap sample. For each of the bootstrap replications, we obtain a corresponding result for P_f, and finally an empirical probability distribution which reflects the scatter of P_f due to the scatter in the input parameter set (m, σ_0, n, and B). Selecting 5% and 95% quantiles from the P_f distribution, we obtain a 90% confidence interval for P_f.

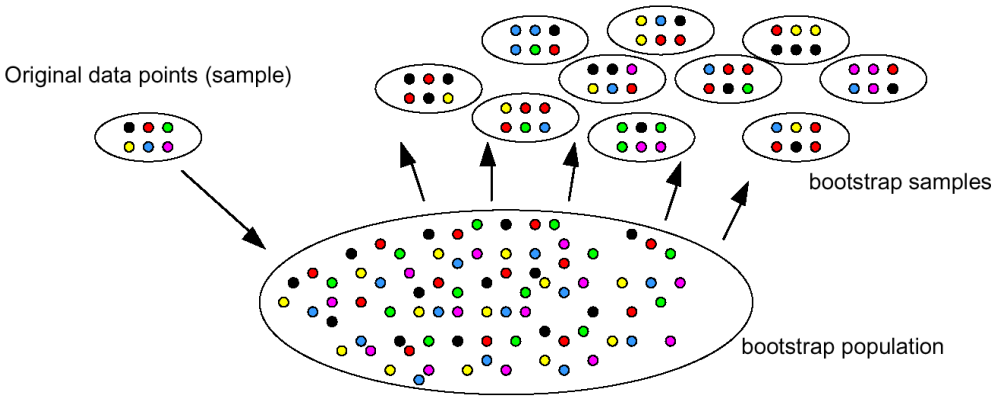

Fig. 1: Bootstrap resampling scheme.

4. EXAMPLES

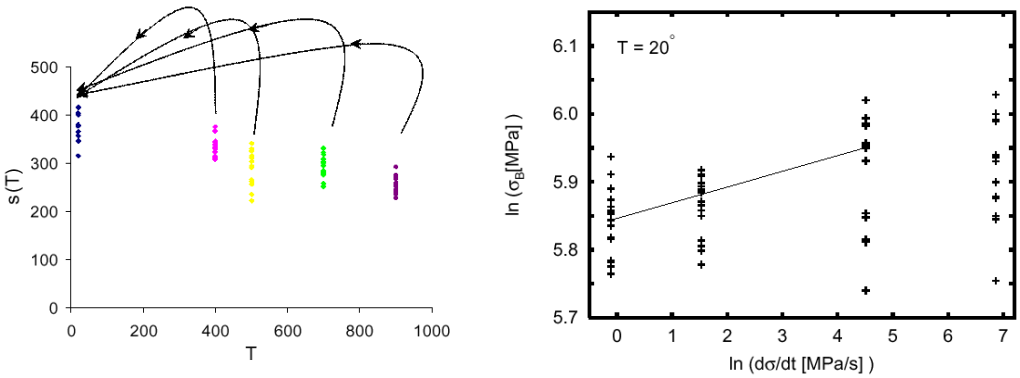

Fig. 2: Experimental data base [8, 11].
a) inert strength results $\sigma(T)$ b) dynamic bending results at room temperature

The data base for both of the following examples consists of five inert strength samples (sample size $N = 15$) at different temperature levels as well as of four samples from dynamic bending tests at various loading rates which are shown in Figs. 2a, b. In the first (toy) example, a four-point bend specimen is considered under sustained loading and the failure probability after 500 h is calculated. Load level and loading time was selected in a way that a moderately high value of P_f was obtained for the original data base. Purpose of this example was to investigate the influence of sample size on the size and stability of the P_f confidence intervals. For this purpose, the inert

strength data from different temperature levels were pooled using a pooling procedure based on a Bayesian Neural Network and all results were transformed into one large (N=75) ambient temperature sample as indicated in Fig 2a. The resulting empirical cumulative distribution function (CDF) for the pooled and unpooled samples together with the corresponding 90% confidence intervals are shown in Fig. 3, where the vertical lines correspond to the P_f -values of the original samples which would have been obtained as result of the analysis using only STAU with no resampling. The results show that a considerable reduction in the broadness of the confidence intervals can be obtained by pooling, which is not surprising because of the increase in the sample size. What surprises, however, is the fact that results from pooled and unpooled samples deviate by a factor of two. But the corresponding upper limits of the 90% confidence intervals are nearly identical thus giving nearly the same reliability in terms of 90% confidence limits by an increase of the failure probability in terms of point estimates from the original samples.

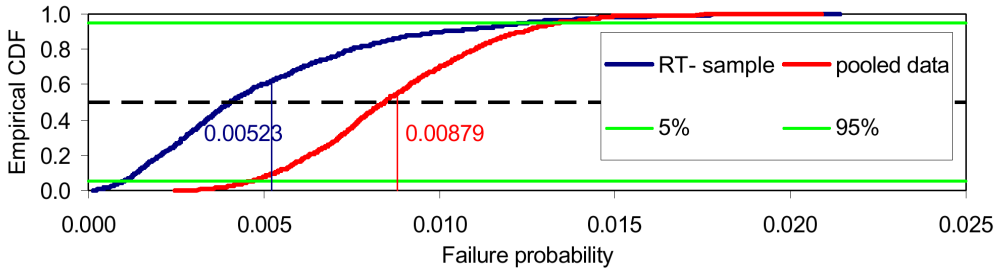

Fig. 3: Empirical CDF of failure probability P_f for pooled and unpooled data.

In the second example, a dry friction test rig is considered where the fracture behaviour of a rotating ceramic disk (Friatec alumina F99,7; d=166mm, t=5mm) is analysed under contact frictional loading of a metallic counterpart made of cast iron (GG25 in German designation) under constant load F_N and constant angular velocity $2\pi f$. The resulting heat flux dQ/dt leads to a large temperature gradient in the vicinity of the frictional surfaces and the resulting thermal stresses may lead to disk fracture. Details of the experimental setup and loading conditions are described in [12]. At constant angular speed, loading was applied during a ramp time t_r = 3s and then kept constant for t_h = 100s before unloading in time t_r was performed. A limit load was observed for (f = 1000 rpm, F_N = 500 N, t_h = 100 s), above which macro-damaging occurred at the outer part of the ceramic disk in the form of fine radial cracks close to the frictional area. With further increase of loading, fragmentation occurs as shown in Fig. 4. For the analysis of the test results, a 2D axisymmetric Finite Element model using ABAQUS 6.4 with about 14000 Elements was developed. Fig. 5 shows a view of the model along a symmetry plane with the ceramic disk (red) and the metallic friction partner (blue) together with the load-bearing carriers. Thermal boundary conditions include heat radiation, convection and conduction at the free surfaces. Mechanical boundary conditions were imposed at the carrier structures. A user subroutine for the friction modelling provides the friction power of the contact surfaces and imposes a corresponding thermal load for each time increment at every node. A coupled thermo-mechanical analysis leads to the resulting stresses. In analogy to the experiment the loading history was in 4 steps: a linear ramp t_r (step 1), a constant load step 2 (t_h); a linear decrease ramp t_r (step 3); time before subsequent cycle (t_h) (step 4). Fig. 6 shows the temperature distribution along the disk surface for the entire cycle of 4 steps; Fig. 7 shows the corresponding distribution of the tangential stress (σ_{33}). R=0 corresponds to the disk centre, R=250 to the disk radius of 83 mm. The tangential stress is dominant and attains its peak

value at the end of the constant load step 2 with $\sigma_{33,max}$ = 180 MPa, whereas radial ($\sigma_{11,max}$ = 40 MPa) and axial ($\sigma_{22,max}$ = 3 MPa) stresses are considerably smaller.

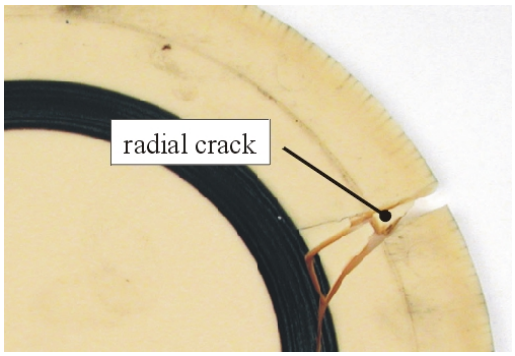

Fig. 4: Macro-damaging of alumina ceramics after frictional load: f = 1000 rpm, F_N = 750 N, t_r = 3s, t_h = 100 s.

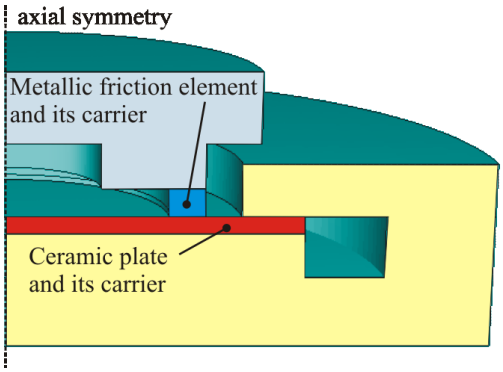

Fig. 5: Section through the finite element model along the symmetry axis

The stress analysis is used for a reliability analysis using the post-processor STAU. A failure probability of P_f = 0.010 is obtained for spontaneous failure after step 2. If sub-critical crack growth is taken into account, P_f = 0.030. Fig. 8 contains these results as vertical bars together with the results of bootstrap resampling as plot of the empirical CDF of $\log_{10}(P_f)$. Taking the CDF quantiles at 5 and 95%, respectively, we obtain 90% confidence intervals for the failure probability for spontaneous fracture (red curve) as [0.0001, 0.11] and for delayed fracture (green curve) as [0.0004, 0.35]. Thus we expect a reasonably large fraction of the specimens to fail in agreement with experimental results. A plot of the local risk of rupture (i.e. the probability density of fracture origin location) in Fig. 9 shows that the most critical region is the outer part of the disk, where according to the fracture appearance shown in Fig. 4 fracture probably initiates.

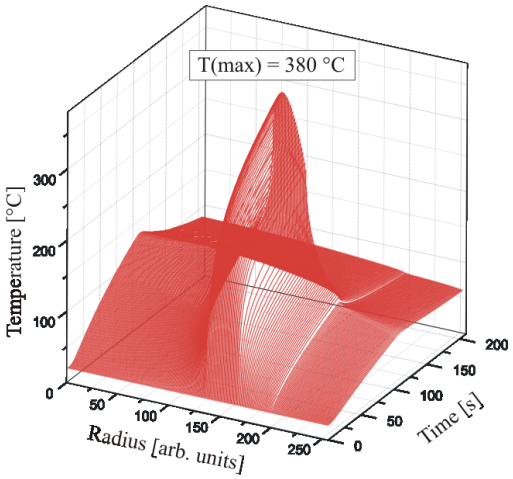

Fig. 6: Temperature distribution for f = 1000 rpm, F_N = 500 N, t_r = 3s, t_h = 100 s

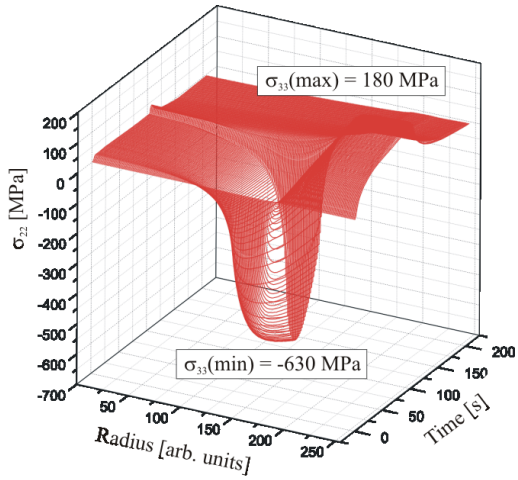

Fig. 7: Tangential stress (σ_{33}) for f = 1000 rpm, F_N = 500 N, t_r = 3s, t_h = 100 s

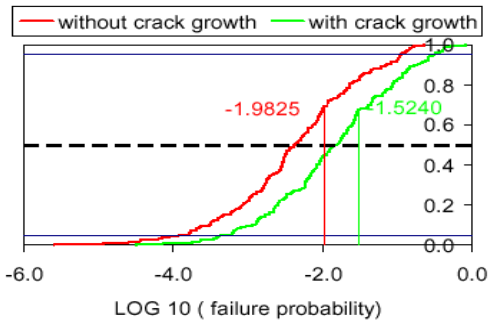

Fig. 8: Empirical CDF for failure probability

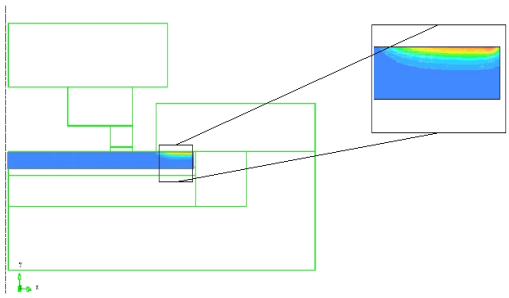

Fig. 9: Local risk of fracture (arbitrary units)

5. CONCLUSIONS

Confidence limits for the failure probability of ceramic components are obtained using the post-processing routine STAU together with bootstrap resampling. For a toy example, pooling led to stable upper bounds for P_f, for a realistic example with friction caused thermo-mechanical loading, predicted confidence intervals and local risk of fracture predictions were in agreement with experimental findings.

ACKNOWLEDGEMENT

Financial support by the "Deutsche Forschungsgemeinschaft" (DFG) is gratefully acknowledged. The work was performed within the framework of the Collaborative Research Centre SFB 483 "High-performance sliding and friction systems based on advanced ceramics".

REFERENCES

[1] S. B. Batdorf and J. G. Crose, A statistical theory for the failure of brittle structures subjected to non-uniform stress, J. Applied Mechanics, **41** (1974), 459-461.

[2] S. B. Batdorf, H. L. Heinisch, Weakest link theory reformulated for arbitrary failure criterion, J. Am. Ceram. Soc., **61** (1978), 355-358.

[3] A. G. Evans, A general approach for the statistical analysis of multiaxial fracture, J. Am. Ceram. Soc., **61** (1978), 302-308.

[4] Y. Matsuo, A probabilistic analysis of brittle fracture loci under bi-axial stress state, Bull. JSME, **24** (1981), 290-294.

[5] A. Brückner-Foit, C. Ziegler, Lifetime prediction for ceramic components subjected to time-dependent loading, Ceramic Engineering and Science Proceedings, **19** (1998), 99-106.

[6] N.N. Nemeth, J. Manderscheid, J. Gyekenyesi, Ceramic Analysis and Reliability Evaluation of Structures (CARES) Manual, NASA TP-2916, Washington D.C:, 1989.

[7] K. Heiermann et al., STAU Vers. 4, User's Manual, Karlsruhe University, 2000.

[8] T. Fett, D. Badenheim, R. Oberacker, K. Heiermann, R. Nejma, Subcritical Crack Growth for an Al_2O_3 Determined with Different Methods, J. Mater. Sci. Letters **22** (2003) 363-365.

[9] D. R. Thoman, L. J. Bain, C. E. Antle, Inferences on the Parameters of the Weibull Distribution, Technometrics, **11**, Nr. 3 (1969) 445 – 460.

[10] B. Efron, R.J. Tibshirani, An Introduction to the Bootstrap, Chapman & Hall/CRC 1998.

[11] K. Heiermann, H. Riesch-Oppermann, N. Huber, Reliability Confidence Intervals for Ceramic Components as Obtained from Bootstrap Methods and Neural Networks, to appear in: Comp. Mat. Sci. (2004).

[12] T. Erbacher, T. Beck, O. Vöhringer: The Behaviour of Alumina Ceramics under Tribological Loading, in: Proc. MaterialsWeek 2002, Mat Info, Frankfurt/Main, 2003.